

## Q-ball imaging using multiple-wavevector fusion

M. H. Khachaturian<sup>1,2</sup>, D. S. Tuch<sup>2,3</sup>

<sup>1</sup>Department of Nuclear Engineering, Massachusetts Institute of Technology, Cambridge, MA, United States, <sup>2</sup>Athinoula A. Martinos Center for Biomedical Imaging, Massachusetts General Hospital, Charlestown, MA, United States, <sup>3</sup>Division of Health Sciences & Technology, Harvard-MIT, Charlestown, MA, United States

**Background** – High angular resolution diffusion imaging (HARDI) methods such as q-ball imaging (QBI) can resolve complex intravoxel structure (1,2). Resolving intravoxel structure with HARDI requires large diffusion wavevectors which substantially reduces the SNR of the HARDI technique. Here we describe a novel diffusion sampling/reconstruction scheme which significantly boosts the SNR of HARDI while retaining the ability to detect intravoxel fiber structure. The method operates by fusing the diffusion signal from two separate measurements acquired with low and high diffusion wavevectors. The multiple wavevector fusion (MWF) procedure provides the benefits of the high SNR at low diffusion wavevectors and the high angular CNR at high wavevectors. The MWF scheme also provides a framework for combining information from DTI and QBI. Numerical simulations show that the MWF method yields significantly more accurate estimates of the true diffusion orientation distribution function (ODF) than a single wavevector QBI acquisition of the same imaging duration. We demonstrate that MWF QBI/DTI of cerebral cortex at 3T reveals more detailed white matter architecture than QBI acquired with only a single diffusion wavevector.

**Theory** – The objective of MWF is to reconstruct the true ODF from multiple ODFs acquired with different diffusion wavevectors. Despite the linear relationship between the diffusion signal and the diffusion ODF (2), optimal combination of multiple wavevectors requires a nonlinear fusion procedure. We consider the problem of fusing low and high wavevector diffusion ODFs, denoted respectively,  $\psi^l$  and  $\psi^h$  acquired with  $q^l$  and  $q^h$ . Each ODF is represented by a common set of spherical basis functions  $\mathbf{Y}$  so that  $\psi^l = \mathbf{Y}\mathbf{w}^l$  and  $\psi^h = \mathbf{Y}\mathbf{w}^h$ . The basis coefficient vectors are denoted  $\mathbf{w}^i = [w_i^j]$  where  $j \in \{h, l\}$ . The true ODF is denoted  $\psi = \mathbf{Y}\mathbf{w}$ . The basis ODFs can be taken as, for example, spherical Gaussian ODFs, spherical harmonics, or spherical wavelets. The basis coefficients for each ODF are estimated by pseudo-inversion of the basis matrix  $\hat{\mathbf{w}}^j = (\mathbf{Y}^H \mathbf{Y})^{-1} \mathbf{Y}^H \psi^j$ . The estimate  $\hat{\mathbf{w}}$  for the true basis vector is derived using the modulus maxima selection rule (3):  $\hat{\mathbf{w}} = [\hat{w}_i] = [w_i^{j(i)}]$  with  $j(i) = \arg \max_{j \in \{h, l\}} |w_i^j|$  where  $|\cdot|$  is the complex modulus. The fused ODF is obtained from the estimated basis vector:  $\hat{\psi} = \mathbf{Y}\hat{\mathbf{w}}$ . The reconstruction performance of MWF QBI compared to linear averaging, single wavevector QBI, and DTI was evaluated by numerical simulation (Fig. 1). MWF QBI demonstrated significantly greater reconstruction accuracy, lower reconstruction variability, and less bias as a function of fiber separation angle.

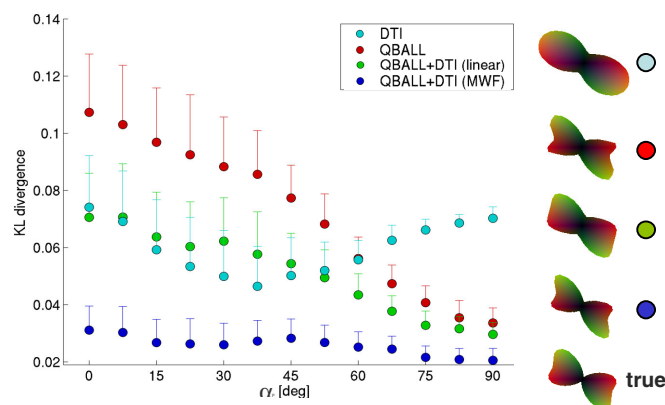


**Fig. 1.** Numerical simulation showing reconstruction error (measured by KL divergence) between reconstructed and true diffusion ODFs for a 2-Gaussian system with principal eigenvector angle separation  $\alpha$ . The ODFs at right are taken from a single trial at  $\alpha=47.5^\circ$ . OBI SNR=2.

**Methods** – Single-shot, EPI DTI and QBI were acquired on a healthy participant on a Siemens Allegra 3T MRI scanner. The DTI parameters were TR/TE=9800/102ms,  $b=700\text{s/mm}^2$ ,  $q=245\text{cm}^{-1}$ , 60 directions (electrostatic shell), 10 T2, 64 axial slices, 2mm isotropic resolution. The QBI imaging parameters were TR/TE=4400/120ms,  $b=4000\text{s/mm}^2$ ,  $q=525\text{cm}^{-1}$ , 492 directions (icosa7), 10 T2, 24 axial slices, 2mm isotropic resolution. The QBI slice prescription was a subset of the DTI prescription. The DTI scan was used as the low-frequency acquisition and the QBI scan as the high-frequency acquisition. To obtain a reduced QBI sampling for comparison, the icosa7 QBI was down-sampled to icosa6 ( $n=362$ ). The DTI and QBI data were fused using the MWF algorithm described above with a spherical Gabor wavelet basis set with  $k=(7^\circ)^{-1}$ ,  $\sigma=60^\circ$  (4). The single-wavevector QBI ( $n=492$ ) was then compared to the MWF of the down-sampled QBI and DTI ( $n=362+70=432$ ).

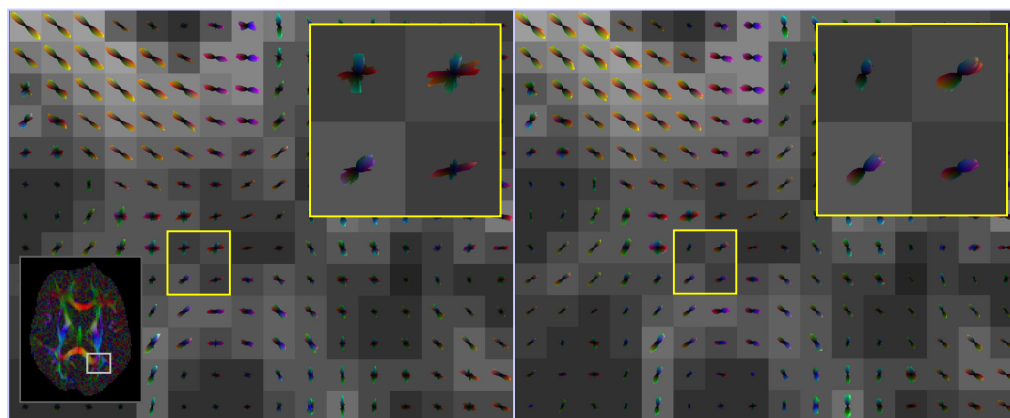


**Fig. 2.** Color-coded diffusion ODF maps for (left) MWF DTI/QBI ( $n=432$ ) and (right) single-wavevector QBI ( $n=492$ ) taken from the projections to the middle and superior occipital gyri.

**Results** – Diffusion ODF maps for single wavevector QBI and MWF DTI/QBI are shown in Fig. 2. The MWF DTI/QBI shows more detailed intravoxel fiber architecture than the single wavevector QBI scan. **Conclusions** – MWF of the diffusion signals from low and high diffusion wavevectors promises to substantially boost the reconstruction accuracy and efficiency of QBI. Future work will investigate the design of more optimal fusion rules, and the performance of MWF QBI at high spatial resolution, and as a function of different diffusion wavevector combinations.

**References** – 1. Tuch, D.S., et al. *Neuron*. 40:885-895, 2003. 2. Tuch, D.S. *Magn Reson Med*. 2004 (in press). 3. Nunez, J., et. al. *IEEE Trans Geosci Remote Sensing*, 37: 1204-1211, 1999. 4. Demanet, L., et. al. *Proc SPIE, Wavelets: Applications in Signal and Image Processing X*, 5207:208-215, 2003.